First-order self-energy correction in hydrogenlike systems

V. A. Yerokhin[1,2,*] and V. M. Shabaev[2]
[1]*Institute for High Performance Computing and Data Bases, Fontanka 118, St. Petersburg 198005, Russia*
[2]*Department of Physics, St. Petersburg State University, Oulianovskaya 1, Petrodvorets, St. Petersburg 198904, Russia*
(Received 23 December 1998)

We present a detailed description of a procedure for the numerical evaluation of the first-order self-energy correction for an arbitrary excited state. An efficient schema of the numerical treatment of the many-potential part of the Dirac-Coulomb Green function improves the speed of the computation considerably. This feature is extremely important for higher-order self-energy calculations. We apply this method to the evaluation of the self-energy correction for the excited states with $|\kappa|\leqslant 5$ and $n\leqslant 5$ for some high-Z ions.
[S1050-2947(99)09907-2]

PACS number(s): 31.30.Jv, 12.20.Ds

INTRODUCTION

The self-energy is the dominant QED effect in atomic structure calculations. While the formula for the bound-state self-energy and the general renormalization scheme have long been understood, the numerical evaluation of this correction for high-Z ions (Z is the nuclear charge number) was a hard problem for a long time. All the calculations made within the αZ expansion (α is the fine-structure constant) fail for these systems, as αZ is valid as an expansion parameter no longer.

The numerical evaluation of the self-energy correction to all orders in αZ has a long history. It is beyond the task of this paper to recite all the authors who contributed to this problem. We mention only a few results here, which are the most important ones in our opinion. The first correct self-energy calculation to all orders in αZ was performed by Desiderio and Johnson [1] for some high-Z ions using a method suggested by Brown, Langer, and Schafaer [2]. Later a method was developed by Mohr [3,4] and a high-precision calculation of the self-energy correction was performed for states in point-nucleus hydrogenic ions with principal quantum numbers $n=1$ and 2. This work was extended to $n=3-5$ for $|\kappa|\leqslant 2$ by Mohr and Kim [5] (κ is the Dirac angular quantum number). The effect of the extended nucleus on the self-energy correction was studied by Mohr and Soff [6]. The method of the potential expansion of the bound-electron propagator for the calculation of the self-energy correction was developed by Snyderman [7] and numerically realized by Blundell and Snyderman [8]. Recently the method of the partial-wave renormalization was developed for the self-energy calculations by Persson, Lindgren, and Salomonson [9] and by Quiney and Grant [10].

In this work we present a procedure for the numerical evaluation of the first-order self-energy correction which is closely related to the methods of Snyderman [7] and Mohr [3], and is applicable for an arbitrary excited state. The present schema differs from the method of Snyderman in the treatment of the many-potential part which is the most time-consuming part of the calculation. A highly efficient procedure is developed for a numerical evaluation of the many-potential part of the Coulomb-Dirac Green function which is expressed in terms of the Whittaker functions and their derivatives. The usage of this procedure and the good convergence efficiency of the resulting partial-wave decomposition simplify the numerical evaluation considerably. The calculation of the self-energy correction for the ground state of hydrogenlike uranium up to a relative precision of 10^{-5} takes only $1\frac{1}{2}$ h on a Pentium with a 100-MHz processor. This feature makes the approach a good basis for higher-order self-energy calculations. The method was successfully applied to calculations of the self-energy screening corrections [11] and the self-energy corrections to the hyperfine splitting [12].

I. BASIC FORMALISM

The energy shift of an electron in a bound state ψ_a due to the first-order self-energy correction is given by the real part of the expression[1]

$$\Delta E_a = 2i\alpha \int_{C_F} d\omega \int d^3\mathbf{x}_1 \int d^3\mathbf{x}_2 \psi_a^\dagger(\mathbf{x}_1)\alpha_\mu \times G(\varepsilon_a-\omega,\mathbf{x}_1,\mathbf{x}_2)\alpha_\nu \psi_a(\mathbf{x}_2) D^{\mu\nu}(\omega,\mathbf{x}_{12}) - \delta m \int d^3\mathbf{x}\,\overline{\psi}_a(\mathbf{x})\psi_a(\mathbf{x}), \quad (1)$$

where $\alpha_\mu=(1,\boldsymbol{\alpha})$, $\boldsymbol{\alpha}$ are the Dirac matrices, the bar over the wave function denotes the Dirac adjoint $\overline{\psi}_a(\mathbf{x})=\psi_a^\dagger(\mathbf{x})\gamma_0$, δm is the mass counterterm, $G(\omega,\mathbf{x}_1,\mathbf{x}_2)=1/(\omega-\mathcal{H})$ is the Dirac-Coulomb Green function, and $\mathcal{H}=(\boldsymbol{\alpha}\cdot\mathbf{p})+\beta m+V(\mathbf{x})$ is the Dirac-Coulomb Hamiltonian. The function $\psi_a(\mathbf{x})$ is the bound solution of the Dirac equation $[\mathcal{H}\psi_a(\mathbf{x})=\varepsilon_a\psi_a(\mathbf{x})]$ written in the form

*Electronic address: yerokhin@pcqnt1.phys.spbu.ru

[1]Relativistic units are used in this paper ($\hbar=c=m=1$). We use roman style (p) for four vectors, bold face ($\mathbf{p}$) for three vectors, and italic style (p) for scalars. Four vectors have the form $\mathrm{p}=(\mathrm{p}_0,\mathbf{p})$. The scalar product of two four vectors is $(\mathrm{p}\cdot\mathrm{k})=\mathrm{p}_0\mathrm{k}_0-(\mathbf{p}\cdot\mathbf{k})$. We use the notations $\not{\mathrm{p}}=\mathrm{p}_\mu\gamma^\mu$, $\hat{\mathbf{p}}=\mathbf{p}/|\mathbf{p}|$.

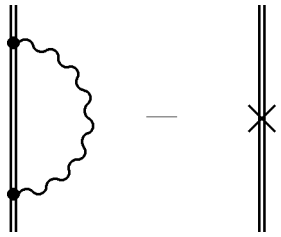

FIG. 1. First-order self-energy correction. The double line denotes the bound-electron propagator, and the cross indicates the mass counterterm.

$$\psi_a(\mathbf{x})=\begin{pmatrix} g_a(x)\chi_{\kappa_a m_a}(\hat{\mathbf{x}}) \\ i f_a(x)\chi_{-\kappa_a m_a}(\hat{\mathbf{x}}) \end{pmatrix}, \tag{2}$$

where $\chi_{\kappa\mu}(\hat{\mathbf{x}})$ is the spin-angular spinor [13]. The function $D^{\mu\nu}(\omega,\mathbf{x}_{12})$ denotes the photon propagator. In this paper we work in the Feynman gauge, thus the photon propagator can be written as

$$D_{\mu\nu}(\omega,\mathbf{x}_{12})=g_{\mu\nu}\frac{\exp[i\sqrt{\omega^2+i\delta}|\mathbf{x}_{12}|]}{4\pi|\mathbf{x}_{12}|}, \tag{3}$$

where $\mathbf{x}_{12}=\mathbf{x}_1-\mathbf{x}_2$, and the branch of the square root is fixed with the condition $\Im(\sqrt{\omega^2+i\delta})>0$, where δ is small and positive.

The self-energy correction (1) is graphically represented in Fig. 1. The integration contour C_F is shown in Fig. 2. To make expression (1) meaningful one should regularize both parts of it in the same covariant way, separate divergent terms, and then pass to the limit which removes the regularization.

To isolate the ultraviolet divergences in Eq. (1), we expand the Dirac-Coulomb Green function in terms of the free Dirac Green function using the operator identity

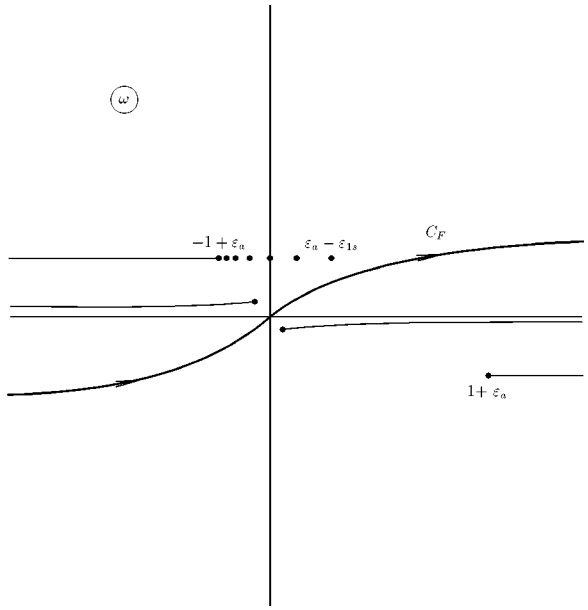

FIG. 2. Contour C_F in the complex ω plane, the singularities, and the branch cuts of the Green function and the photon propagator. ε_a denotes the energy of the initial state.

$$\frac{1}{\omega-\mathcal{H}}=\frac{1}{\omega-\mathcal{H}_0}+\frac{1}{\omega-\mathcal{H}_0}V\frac{1}{\omega-\mathcal{H}_0}+\frac{1}{\omega-\mathcal{H}_0}\times V\frac{1}{\omega-\mathcal{H}}V\frac{1}{\omega-\mathcal{H}_0}, \tag{4}$$

where $\mathcal{H}_0=(\boldsymbol{\alpha}\cdot\mathbf{p})+\beta m$ is the free Dirac Hamiltonian, V denotes the interaction with the nucleus. This expansion is widely used in atomic QED calculations. It was used first by Baranger, Bethe, and Feynman [14] to extract the physical self-energy shift through order $\alpha(\alpha Z)^5$. Whichmann and Kroll [15] employed this method for an evaluation of the vacuum-polarization correction. For the calculation of the self-energy correction in all orders of αZ, this method was developed by Snyderman [7] and numerically realized by Blundell and Snyderman [8].

The three terms in Eq. (4) inserted into Eq. (1) correspond to zero-potential, one-potential, and many-potential terms, respectively. The resulting expansion is graphically represented in Fig. 3. It can be expressed with the first two terms converted into the momentum space as follows:

$$\begin{aligned}\Delta E_a=&\int\frac{d^3\mathbf{p}}{(2\pi)^3}\overline{\psi}_a(\mathbf{p})(\Sigma^{(0)}(\mathrm{p})-\delta m)\psi_a(\mathbf{p})\\&+\int\frac{d^3\mathbf{p}'}{(2\pi)^3}\int\frac{d^3\mathbf{p}}{(2\pi)^3}\overline{\psi}_a(\mathbf{p}')\Gamma^0(\mathrm{p}',\mathrm{p})\\&\times V(|\mathbf{p}'-\mathbf{p}|)\psi_a(\mathbf{p})\\&+2i\alpha\int_{C_F}d\omega\int d^3\mathbf{x}_1\int d^3\mathbf{x}_2\psi_a^\dagger(\mathbf{x}_1)\alpha_\mu\\&\times G^{2+}(\varepsilon_a-\omega,\mathbf{x}_1,\mathbf{x}_2)\alpha_\nu\psi_a(\mathbf{x}_2)D^{\mu\nu}(\omega,\mathbf{x}_{12}),\end{aligned} \tag{5}$$

where $\varepsilon_a=\mathrm{p}_0=\mathrm{p}_0'$, $\Sigma^{(0)}(\mathrm{p})$ is the free-electron self-energy operator defined in Appendix A, $\Gamma^0(\mathrm{p}',\mathrm{p})$ is the time component of the free-electron vertex operator defined in Appendix B, and $\psi_a(\mathbf{p})$ is the Fourier transform of the coordinate-space wave function (2):

$$\psi_a(\mathbf{p})=\int d^3\mathbf{x}\,e^{-i\mathbf{p}\mathbf{x}}\psi_a(\mathbf{x})=i^{-l_a}\begin{pmatrix}\tilde{g}_a(p)\chi_{\kappa_a m_a}(\hat{\mathbf{p}})\\ \tilde{f}_a(p)\chi_{-\kappa_a m_a}(\hat{\mathbf{p}})\end{pmatrix}. \tag{6}$$

$l_a=|\kappa_a+1/2|-1/2$. The G^{2+} function denotes a part of the electron propagator containing two or more Coulomb interactions with the nucleus

$$G^{2+}(\omega)=\frac{1}{\omega-\mathcal{H}_0}V\frac{1}{\omega-\mathcal{H}}V\frac{1}{\omega-\mathcal{H}_0}. \tag{7}$$

It can be easily shown that the many-potential term does not contain any divergences. After the isolation of ultraviolet divergences in the zero- and one-potential terms (see Appendixes A and B), one can obtain

$$\Sigma^{(0)}(\mathrm{p})=\delta m-\frac{\alpha}{4\pi}\Delta_\epsilon(\not{p}-m)+\Sigma_R^{(0)}(\mathrm{p}), \tag{8}$$

$$\Gamma^{\mu}(\mathrm{p}',\mathrm{p})=\frac{\alpha}{4\pi}\Delta_{\epsilon}\gamma^{\mu}+\Gamma_{R}^{\mu}(\mathrm{p}',\mathrm{p}).$$

Using the Fourier transformed Dirac equation

$$(\not{p}-m)\psi_a(\mathbf{p})=\int\frac{d^3\mathbf{p}'}{(2\pi)^3}\gamma^0 V(|\mathbf{p}-\mathbf{p}'|)\psi_a(\mathbf{p}'), \quad (9)$$

one can see the explicit cancellation of the ultraviolet divergences between the zero- and one-potential terms in Eq. (5).

As a result, we express the self-energy correction ΔE_a as the sum of the three finite terms:

$$\Delta E_a=\Delta E_{\mathrm{zero}}+\Delta E_{\mathrm{one}}+\Delta E_{\mathrm{many}}, \quad (10)$$

$$\Delta E_{\mathrm{zero}}=\int\frac{d^3\mathbf{p}}{(2\pi)^3}\,\overline{\psi}_a(\mathbf{p})\Sigma_R^{(0)}(\mathrm{p})\psi_a(\mathbf{p}), \quad (11)$$

$$\Delta E_{\mathrm{one}}=\int\frac{d^3\mathbf{p}'}{(2\pi)^3}\int\frac{d^3\mathbf{p}}{(2\pi)^3}\,\overline{\psi}_a(\mathbf{p}')\Gamma_R^0(\mathrm{p}',\mathrm{p})\times V(|\mathbf{p}'-\mathbf{p}|)\psi_a(\mathbf{p}), \quad (12)$$

$$\Delta E_{\mathrm{many}}=2i\alpha\int_{C_F}d\omega\int d^3\mathbf{x}_1\int d^3\mathbf{x}_2\psi_a^{\dagger}(\mathbf{x}_1)\alpha_{\mu}\times G^{2+}(\varepsilon_a-\omega,\mathbf{x}_1,\mathbf{x}_2)\alpha_{\nu}\psi_a(\mathbf{x}_2)D^{\mu\nu}(\omega,\mathbf{x}_{12}). \quad (13)$$

II. ZERO- AND ONE-POTENTIAL TERMS

The angular integration in Eq. (11) can be easily performed using the expression for the free self-energy operator (A5) and the relation

$$(\boldsymbol{\sigma}\cdot\hat{\mathbf{p}})\chi_{\kappa\mu}(\hat{\mathbf{p}})=-\chi_{-\kappa\mu}(\hat{\mathbf{p}}). \quad (14)$$

The result of the angular integration is

$$\Delta E_{\mathrm{zero}}=\frac{\alpha}{4\pi}\int_0^{\infty}\frac{p^2dp}{(2\pi)^3}\{a(\rho)[\tilde{g}_a^2(p)-\tilde{f}_a^2(p)]+b(\rho)\times[\varepsilon_a(\tilde{g}_a^2(p)+\tilde{f}_a^2(p))+2p\tilde{g}_a(p)\tilde{f}_a(p)]\}. \quad (15)$$

Here $p=|\mathbf{p}|$, the functions $a(\rho)$ and $b(\rho)$ are defined by Eq. (A6) and (A7), and $\tilde{g}_a(p)$ and $\tilde{f}_a(p)$ are the components of the momentum-space wave function (6).

The one-potential term is given by expression (12). The Coulomb potential in the momentum space is

$$V(|\mathbf{p}-\mathbf{p}'|)=-4\pi\frac{\alpha Z}{(\mathbf{p}-\mathbf{p}')^2}. \quad (16)$$

The angular integration can be easily performed using expression (B18) and the following relation:

$$\frac{1}{2j+1}\sum_{\mu}\chi_{\kappa\mu}^{\dagger}(\hat{\mathbf{p}}')\chi_{\kappa\mu}(\hat{\mathbf{p}})=\frac{1}{4\pi}P_l(\xi), \quad (17)$$

where $\xi=\cos(\widehat{\mathbf{pp}'})$, $j=|\kappa|-1/2$, $l=|\kappa+\frac{1}{2}|-\frac{1}{2}$, and $P_l(\xi)$ is a Legendre polynomial. As a result, we have

$$\Delta E_{\mathrm{one}}=-\frac{\alpha^2Z}{32\pi^5}\int_0^{\infty}dp'\int_0^{\infty}dp\int_{-1}^{1}d\xi\frac{p'^2p^2}{q^2}\times\{\mathcal{F}_1(p',p,\xi)P_l(\xi)+\mathcal{F}_2(p',p,\xi)P_{\bar{l}}(\xi)\}, \quad (18)$$

where $p=|\mathbf{p}|$, $p'=|\mathbf{p}'|$, $\bar{l}=2j-l$, and $q^2=p^2+p'^2-2pp'\xi$, and the functions $\mathcal{F}_1$ and $\mathcal{F}_2$ are given by Eqs. (B19) and (B20).

III. MANY-POTENTIAL TERM

The many-potential term is given by expression (13), with the integration contour shown in Fig. 2. The integrand is an analytic function of ω, except for the poles of the Green function ($\omega=\varepsilon_a-\varepsilon_n+i0$, where index n runs over all bound states and ε_a is the energy of the initial state), its branch points [$\omega=\varepsilon_a\pm(1-i0)$], and the branch points of the photon propagator ($\omega=\pm\sqrt{-i\delta}$). The singularities and the branch cuts of the Green function and the photon propagator are shown in Fig. 2.

For the numerical evaluation of the integral over ω, we deform the integration contour C_F in a way shown in Fig. 4, and divide the integral into two parts which correspond to integrations over two parts C_L and C_H of the new contour. We refer to these parts as the *low-energy* and the *high-energy* terms, respectively. The contour C_L is chosen in a way to avoid singularities which come from the bound states with the energy $\varepsilon_n<\varepsilon_a$. This choice allows the procedure to be applicable to an arbitrary initial bound state. The contour C_H extends from $-i\infty+\varepsilon_0$ to ε_0 and from ε_0 to $i\infty+\varepsilon_0$. It is chosen in a way to eliminate strong oscillations arising in the high-energy region of the contour C_F in favor of exponentially decaying integrands. One can see that the integrand in Eq. (13) falls off so rapidly that the contribution of the big quarter circles of the deformed contour in Fig. 4 vanishes as their radius goes to infinity.

This choice of the integration contour is similar to the one used by Mohr [3]. It differs by the fact that the contour C_L extends in the complex plane rather than along the real axis, and by the choice of the parameter ε_0. However, one should stress the difference between the approach described here and the method of Mohr. In Ref. [3] the self-energy correction was divided into low- and high-energy parts first, and then the subtraction of ultraviolet divergences was performed in the high-energy part. We divide only the many-potential term into low- and high-energy parts. As a result, we obtain a partial-wave expansion which converges faster than the one in Ref. [3].

An advantage of the bending of the integration contour C_L into the complex plane is clear for highly-excited states. If the contour C_L extends along the real axis, as in Refs. [3, 5], one has to evaluate numerically the principal value of an integral containing as many singularities as the number of the bound states n with the energy $\varepsilon_n<\varepsilon_a$.

The contour C_L consists of two parts: one extends along the upper bank of the cut of the photon propagator, and the other extends along the lower bank. Each part of the contour is chosen to be a half of an ellipse,

$$\omega=\frac{\varepsilon_0}{2}\left(1+\frac{\Delta e^{-i\varphi}}{\sqrt{\Delta^2\cos^2\varphi+\sin^2\varphi}}\right), \tag{19}$$

where $\varphi=0,\ldots,\pi$ corresponds to the lower part of the contour and $\varphi=\pi,\ldots,0$ to the upper part. One should note that the integrand in Eq. (13) on the upper and lower banks of the cut differs only by the sign of the argument of the exponent in the photon propagator. The variables ε_0 and Δ are free parameters which were adjusted empirically to achieve the best numerical efficiency of the algorithm. The value of Δ should not be large, because the photon propagator on the upper bank of the cut is an exponentially growing function in the lower half of the complex ω plane which can cause numerical difficulties. For practical calculations we use $\varepsilon_0=\varepsilon_a-0.9\varepsilon_{1s}$, $\Delta=\varepsilon_a/(5n^{1/3})$, where n is the principal quantum number of the initial state, and ε_{1s} is the energy of the ground state.

Let us consider the evaluation of the angular integrals in Eq. (13). For this purpose we use the spectral representation of the Green function $G^{2+}(\omega,\mathbf{x}_1,\mathbf{x}_2)$,

$$G^{2+}(\omega,\mathbf{x}_1,\mathbf{x}_2)=\sum_i\frac{\phi_i^{(+)}(\omega,\mathbf{x}_1)[\phi_i^{(-)}(\omega,\mathbf{x}_2)]^\dagger}{\omega-\varepsilon_i(1-i0)}, \tag{20}$$

where $\phi_i^{(\pm)}(\omega,\mathbf{x})$ is given by

$$\phi_i^{(\pm)}(\omega,\mathbf{x})=(\omega-\mathcal{H}_0(1\mp i0))^{-1}V(x)\psi_i(\mathbf{x}), \tag{21}$$

and i runs over all solutions $\psi_i(\mathbf{x})$ of the Dirac-Coulomb equation: $\mathcal{H}\psi_i(\mathbf{x})=\varepsilon_i\psi_i(\mathbf{x})$. One can easily see that the angular dependence of $G^{2+}(\omega,\mathbf{x}_1,\mathbf{x}_2)$ is the same as for the Dirac-Coulomb Green function $G(\omega,\mathbf{x}_1,\mathbf{x}_2)$.

After substitution of Eq. (20) into Eq. (13) and the deformation of the integration contour, we have

$$\Delta E_{\rm many}=2i\alpha\sum_i\int_{C_L+C_H}d\omega\times\frac{\langle a\phi_i^{(-)}|\alpha_\mu\alpha_\nu D^{\mu\nu}(\omega)|\phi_i^{(+)}a\rangle}{\varepsilon_a-\omega-\varepsilon_i}. \tag{22}$$

To perform the angular integration, we introduce the function $R_L(\omega,abcd)$ in the following way [16]:

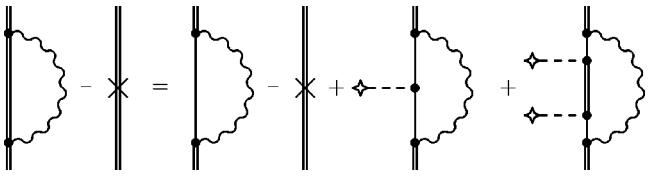

FIG. 3. Decomposition of the bound-state self-energy into zero-potential, one-potential, and many-potential terms. Single lines represent free-electron propagators, double lines bound-electron propagators, and dashed lines the binding potential. The cross represents the mass counterterm.

$$4\pi\langle ab|\alpha_\mu\alpha_\nu D^{\mu\nu}(\omega)|cd\rangle=\sum_{J=0}^{\infty}I_J(abcd)R_J(\omega,abcd), \tag{23}$$

where the function $I_J(abcd)$ contains the whole dependence on the moment projections:

$$I_J(abcd)=\sum_{m_J}(-1)^{j_a-m_a+J-m_J+j_b-m_b}\times\begin{pmatrix}j_a & J & j_c\\ -m_a & m_J & m_c\end{pmatrix}\begin{pmatrix}j_b & J & j_d\\ -m_b & -m_J & m_d\end{pmatrix}. \tag{24}$$

The expression for the radial integral $R_J(\omega,abcd)$ is given in Appendix C.

After summing over the moment projections of the intermediate states, one can obtain

$$\Delta E_{\rm many}=\frac{i\alpha}{2\pi}\sum_{\kappa_i,n_i}\frac{(-1)^{j_i-j_a}}{2j_a+1}\times\int_{C_L+C_H}d\omega\frac{\sum_J(-1)^J R_J(\omega,a\phi_i^{(-)}\phi_i^{(+)}a)}{\varepsilon_a-\omega-\varepsilon_i}, \tag{25}$$

where κ_i is the Dirac angular quantum number of the intermediate states ϕ_i, n_i is the principal quantum number, $j_i=|\kappa_i|-\frac{1}{2}$, and the summing over J extends from $J=|j_i-j_a|$ up to $J=j_i+j_a$.

Expressing Eq. (25) in terms of the Green function, it is easy to obtain

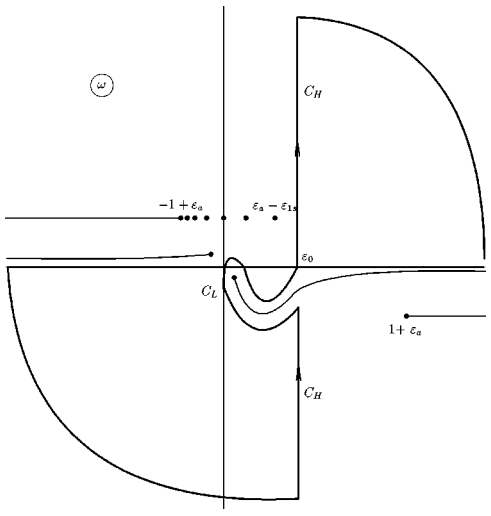

FIG. 4. Deformed contour in the complex ω plane, the singularities, and the branch cuts of the Green function and the photon propagator. The new contour is divided into two parts C_L and C_H, which correspond to the low- and high-energy parts, respectively.

TABLE I. First-order self-energy correction for the hydrogenlike point-nucleus tungsten, bismuth, and uranium expressed in terms of the function $F(\alpha Z)$ defined by Eq. (32).

	$d_{5/2}$			$f_{5/2}$		$f_{7/2}$		$g_{7/2}$	$g_{9/2}$
Z	$n=3$	$n=4$	$n=5$	$n=4$	$n=5$	$n=4$	$n=5$	$n=5$	$n=5$
74	0.0550(0)	0.0598(4)	0.0628(6)	−0.0198(4)	−0.0184(7)	0.0231(4)	0.0247(7)	−0.0121(9)	0.0135(9)
83	0.0583(0)	0.0639(3)	0.0671(5)	−0.0194(3)	−0.0180(5)	0.0238(3)	0.0254(6)	−0.0121(8)	0.0136(8)
92	0.0620(0)	0.0684(2)	0.0719(5)	−0.0189(2)	−0.0175(5)	0.0245(2)	0.0262(5)	−0.0121(5)	0.0136(6)

$$\Delta E_{\rm many}=\frac{i\alpha}{2\pi}\frac{1}{2j_a+1}\sum_{|\kappa_i|=1}^{\infty}\int_{C_L+C_H}d\omega \times\int_0^\infty x_1^2dx_1\int_0^\infty x_2^2dx_2\sum_{\substack{\mathrm{sign}(\kappa_i)\\ J}}(2J+1) \times\left\{[C_J(\kappa_i,\kappa_a)]^2g_J(\omega)\{\mathbf{G}^{2+}_{\kappa_i}\}^I_{aa}-\sum_{L=J-1}^{J+1}g_L(\omega) \times\{\mathbf{G}^{2+}_{\kappa_i}\}^{II,aa}_{\kappa_i\kappa_i,JL}\right\}, \tag{26}$$

where $g_L(\omega)=g_L(\omega,x_<,x_>)$ is defined by Eq. (C6), and $\mathbf{G}^{2+}_\kappa=\mathbf{G}^{2+}_\kappa(\varepsilon_a-\omega,x_1,x_2)$ is the radial part of the $G^{2+}(\varepsilon_a-\omega,\mathbf{x}_1,\mathbf{x}_2)$ function defined in Appendix D. Other notations used in Eq. (26) are as follows:

$$\{\mathbf{A}\}^I_{ab}=g_a(x_1)A_{11}g_b(x_2)+g_a(x_1)A_{12}f_b(x_2) +f_a(x_1)A_{21}g_b(x_2)+f_a(x_1)A_{22}f_b(x_2), \tag{27}$$

$$\{\mathbf{A}\}^{II,ab}_{\kappa_1\kappa_2,JL}=f_a(x_1)A_{11}f_b(x_2)S_{JL}(-\kappa_a,\kappa_1)S_{JL}(-\kappa_b,\kappa_2) -f_a(x_1)A_{12}g_b(x_2)S_{JL}(-\kappa_a,\kappa_1)S_{JL}(\kappa_b,-\kappa_2) -g_a(x_1)A_{21}f_b(x_2)S_{JL}(\kappa_a,-\kappa_1)S_{JL}(-\kappa_b,\kappa_2) +g_a(x_1)A_{22}g_b(x_2)S_{JL}(\kappa_a,-\kappa_1)S_{JL}(\kappa_b,-\kappa_2), \tag{28}$$

where the angular coefficients C_J and S_{JL} are defined by Eqs. (C7)–(C10).

IV. NUMERICAL DETAILS

For the numerical evaluation of all the integrals, we use the Gauss-Legendre quadratures. Computation of the bound-state wave functions in the coordinate and in the momentum space was performed following Ref. [17]. While the integration of the zero-potential term is straightforward, the one-potential term requires some care. For its calculation one has to evaluate a four-dimensional integral numerically [a three-dimensional integration in Eq. (18) and an additional integration over the Feynman parameter in Eqs. (B12)–(B15)]. One can see that the integrand in Eq. (18) has an integrable singularity when $q=0$. To handle the singularity, it is convenient to make the change of variables $\{pp'\xi\}\to\{xyq\}$, where

$$x=p+p', \tag{29}$$

$$y=p-p', \tag{30}$$

$$q=\sqrt{p^2+p'^2-2pp'\xi}. \tag{31}$$

The many-potential term was evaluated dividing the contour of the integration into two pieces C_L and C_H corresponding to the low- and high-energy terms, as discussed in Sec. III. The numerical evaluation of the integrals over $x_{1,2}$ in the both terms was performed in the same way using the change of the variables [3] $\{x_1x_2\}\to\{ry\}$, where $r=x_</x_>$, $y=2\alpha Zx_>$. The numerical evaluation of the integrand is based on the computation of the $\mathbf{G}^{2+}_\kappa(\omega,x_1,x_2)$ function described in detail in Appendix D.

In contrast to the method of Mohr, we perform all the integrations before the summing over $|\kappa|$ is evaluated. As a result, after all the integrations are completed, we have a smooth $|\kappa|$ series which can be easily extrapolated. The expansion of the low-energy part usually converges very well (faster than $|\kappa|^{-3}$), and it can be summed up to a desirable precision without any extrapolation. The maximal value of $|\kappa|$ used in the most difficult case considered here ($n=5$) is 35, while for the ground state the sum can be terminated already at $|\kappa|=5$. The high-energy term is usually smaller by an order of magnitude than the low-energy part, but its convergency is slower ($|\kappa|^{-3}$ for high $|\kappa|$). The summation was terminated at $|\kappa|=50$ or less, and the remainder of the series was estimated using a polynomial fitting in $1/|\kappa|$.

The results of the calculations of the first-order self-energy corrections for the hydrogenlike point-nucleus tungsten, bismuth, and uranium are presented in Table I for states with $3\leqslant|\kappa|\leqslant5$ and $n\leqslant5$. We express our results in terms of the function $F(\alpha Z)$:

$$\Delta E_a=\frac{\alpha}{\pi}\frac{(\alpha Z)^4}{n^3}F(\alpha Z)mc^2. \tag{32}$$

In Table II we compare our calculations with the most precise results obtained by Mohr and Kim [5] and Indelicato and Mohr [18].

One should note that a numerical cancellation between different contributions to the self-energy correction arises which appears to be much stronger for highly excited states than for low-lying ones. To illustrate this, in Table III we give a breakdown for the different terms of the self-energy correction for $1s_{1/2}$ and $5g_{9/2}$ states of the hydrogenlike uranium.

TABLE II. Comparison of the present results with the previous calculations for $Z=90$ in terms of the function $F(\alpha Z)$ defined by Eq. (32).

	$p_{3/2}$				$d_{3/2}$		
Ref.	$n=2$	$n=3$	$n=4$	$n=5$	$n=3$	$n=4$	$n=5$
This work	0.29066(3)	0.33500(5)	0.3507(3)	0.3578(7)	−0.02249(5)	−0.0149(2)	−0.0105(5)
[5]		0.3350(1)	0.3507(1)	0.3574(1)	−0.0225(1)	−0.0149(1)	−0.0108(1)
[18]	0.29066783(1)	0.33496587(8)			−0.02248223(3)		

CONCLUSION

What we have presented in this paper is a practical highly efficient procedure for the numerical evaluation of the first-order self-energy correction for an arbitrary excited state. In this paper we discuss only the point-nucleus problem. The procedure can be immediately extended to the finite-nucleus case. We performed calculations of the self-energy correction for low-lying excited states employing the hollow-shell nuclear model, and obtained a good agreement with the results of Mohr and Soff [6].

At present there are different methods developed for the calculation of the first-order self-energy correction; some of them were mentioned in the Introduction. Most of these methods can be adopted for the calculation of the self-energy in an arbitrary spherically symmetric potential. However, some problems may arise in the extension of a method for *ab initio* higher-order self-energy calculations. For instance, the method of the partial-wave renormalization applied to the two-electron self-energy correction gives a small spurious term due to a noncovariant renormalization procedure (see Ref. [11] and references therein). In this paper we have presented a covariant procedure for the calculation of the first-order self-energy which has been proven to be a very efficient basis for calculations of higher-order self-energy corrections [11,12].

ACKNOWLEDGMENTS

Valuable conversations with Thomas Beier are gratefully acknowledged. This work was supported by the Russian Foundation for Basic Research (Grant No. 98-02-18350), and by the program ''Russian Universities Basic Research'' (Project No. 3930).

APPENDIX A: FREE ELECTRON SELF-ENERGY OPERATOR

The free-electron self-energy operator in the Feynman gauge is given by the integral

TABLE III. Various contributions to the self-energy correction for $1s_{1/2}$ and $5g_{9/2}$ states of the hydrogenlike uranium ($Z=92$) in atomic units.

Contribution	$1s_{1/2}$	$5g_{9/2}$
Zero-potential term	−19.1010	−2.67403
One-potential term	17.5809	1.94711
Low-energy term	2.7815	0.71305
High-energy term	11.9500(2)	0.01484(4)
Total self-energy	13.2114(2)	0.00097(4)

$$\Sigma^{(0)}(\mathrm{p})=-4\pi i\alpha\int\frac{d^4\mathrm{k}}{(2\pi)^4}\frac{1}{\mathrm{k}^2}\gamma_\sigma\frac{\not{\mathrm{p}}-\not{\mathrm{k}}+m}{(\mathrm{p}-\mathrm{k})^2-m^2}\gamma^\sigma. \tag{A1}$$

This expression is infrared finite, and we can use the photon propagator with the zero photon mass already from the beginning. Expression (A1) is obviously ultraviolet divergent. It can be shown that this divergency is only logarithmical, if the covariant regularization is used. In our calculation we use the dimensional regularization

$$\frac{d^4\mathrm{k}}{(2\pi)^4}\to\frac{d^D\mathrm{k}}{(2\pi)^D}, \tag{A2}$$

with $D=4-2\epsilon$.

To separate the ultraviolet divergency, we write the self-energy operator in the form

$$\Sigma^{(0)}(\mathrm{p})=\delta m-\frac{\alpha}{4\pi}\Delta_\epsilon(\not{p}-m)+\Sigma_R^{(0)}(\mathrm{p}), \tag{A3}$$

where $\delta m=3\alpha/(4\pi)m(\Delta_\epsilon+\frac{4}{3})$ is the counterterm of the mass renormalization, $\Delta_\epsilon=(1/\epsilon)-\gamma_E+\ln 4\pi-\ln m^2$, and γ_E is the Euler constant. We prefer to write the self-energy operator in form (A3) rather than in the more usual one:

$$\Sigma^{(0)}(\mathrm{p})=\delta m+(Z_2-1)(\not{p}-m)+\Sigma_{\mathrm{ren}}^{(0)}(\mathrm{p}). \tag{A4}$$

The reason for this is that the wave-function renormalization constant Z_2 is infrared divergent in the Feynman gauge, and its separation causes infrared divergences in $\Sigma_{\mathrm{ren}}^{(0)}(\mathrm{p})$. In Eq. (A3) we separate only the ultraviolet divergent part of Z_2, and $\Sigma_R^{(0)}(\mathrm{p})$ does not contain any divergences.

The $\Sigma_R^{(0)}(\mathrm{p})$ operator in the Feynman gauge can be easily calculated to be

$$\Sigma_R^{(0)}(\mathrm{p})=\frac{\alpha}{4\pi}(a(\rho)+\not{p}b(\rho)), \tag{A5}$$

$$a(\rho)=2m\left(1+\frac{2\rho}{1-\rho}\ln\rho\right), \tag{A6}$$

$$b(\rho)=-\frac{2-\rho}{1-\rho}\left(1+\frac{\rho}{1-\rho}\ln\rho\right), \tag{A7}$$

where $\rho=(m^2-\mathrm{p}^2)/m^2$.

APPENDIX B: FREE-ELECTRON VERTEX OPERATOR

The free-electron vertex operator in the Feynman gauge is given by

$$\Gamma^{\mu}(\mathrm{p}',\mathrm{p}) = -4\pi i\alpha \int \frac{d^4\mathrm{k}}{(2\pi)^4}\,\frac{1}{\mathrm{k}^2}\,\gamma_\sigma \frac{\not{\mathrm{p}}'-\not{\mathrm{k}}+m}{(\mathrm{p}'-\mathrm{k})^2-m^2} \times \gamma^{\mu}\frac{\not{\mathrm{p}}-\not{\mathrm{k}}+m}{(\mathrm{p}-\mathrm{k})^2-m^2}\,\gamma^{\sigma}. \tag{B1}$$

Expression (B1) is infrared finite. It contains the logarithmic ultraviolet divergency which is handled using the dimensional regularization with $D=4-2\epsilon$ as in the case of the free self-energy operator. The evaluation of the free-electron vertex operator can be found in Ref. [7]. Here we present only the final expressions suitable for the numerical evaluation, correcting a number of misprints in Ref. [7].

We separate the ultraviolet divergency in $\Gamma^{\mu}(\mathrm{p}',\mathrm{p})$ in the following way:

$$\Gamma^{\mu}(\mathrm{p}',\mathrm{p}) = \frac{\alpha}{4\pi}\Delta_\epsilon \gamma^{\mu} + \Gamma^{\mu}_R(\mathrm{p}',\mathrm{p}), \tag{B2}$$

where $\Delta_\epsilon = (1/\epsilon) - \gamma_E + \ln 4\pi - \ln m^2$. Again, we remark that in Eq. (B2) we separate only the ultraviolet divergent part of the renormalization constant Z_1.

The $\Gamma^{\mu}_R(\mathrm{p}',\mathrm{p})$ function is finite, and can be evaluated to be

$$\Gamma^{\mu}_R(\mathrm{p}',\mathrm{p}) = \frac{\alpha}{4\pi}\{A\gamma^{\mu} + \not{\mathrm{p}}'(B_1\mathrm{p}'^{\mu} + B_2\mathrm{p}^{\mu}) + \not{\mathrm{p}}(C_1\mathrm{p}'^{\mu} + C_2\mathrm{p}^{\mu}) + D(\not{\mathrm{p}}'\gamma^{\mu}\not{\mathrm{p}}) + H_1\mathrm{p}'^{\mu} + H_2\mathrm{p}^{\mu}\}, \tag{B3}$$

$$A = C_{24} - 2 + \mathrm{p}'^2 C_{11} + \mathrm{p}^2 C_{12} + 4(\mathrm{p}'\cdot\mathrm{p})(C_0 + C_{11} + C_{12}) + m^2(-2C_0 + C_{11} + C_{12}), \tag{B4}$$

$$B_1 = -4(C_{11} + C_{21}), \tag{B5}$$

$$B_2 = -4(C_0 + C_{11} + C_{12} + C_{23}), \tag{B6}$$

$$C_1 = -4(C_0 + C_{11} + C_{12} + C_{23}), \tag{B7}$$

$$C_2 = -4(C_{12} + C_{22}), \tag{B8}$$

$$D = 2(C_0 + C_{11} + C_{12}), \tag{B9}$$

$$H_1 = 4m(C_0 + 2C_{11}), \tag{B10}$$

$$H_2 = 4m(C_0 + 2C_{12}), \tag{B11}$$

where

$$C_0 = \int_0^1 \frac{dy}{(y\mathrm{p}' + (1-y)\mathrm{p})^2}(-\ln X), \tag{B12}$$

$$\begin{pmatrix} C_{11} \\ C_{12} \end{pmatrix} = \int_0^1 \frac{dy}{(y\mathrm{p}' + (1-y)\mathrm{p})^2}\begin{pmatrix} y \\ 1-y \end{pmatrix}(1 - Y\,\ln X), \tag{B13}$$

$$\begin{pmatrix} C_{21} \\ C_{22} \\ C_{23} \end{pmatrix} = \int_0^1 \frac{dy}{(y\mathrm{p}' + (1-y)\mathrm{p})^2}\begin{pmatrix} y^2 \\ (1-y)^2 \\ y(1-y) \end{pmatrix} \times\left(-\frac{1}{2} + Y - Y^2\ln X\right), \tag{B14}$$

$$C_{24} = -\int_0^1 dy\,\ln(y^2\mathrm{q}^2/m^2 - y\mathrm{q}^2/m^2 + 1), \tag{B15}$$

and

$$X = 1 + \frac{1}{Y}, \tag{B16}$$

$$Y = \frac{m^2 - y\mathrm{p}'^2 - (1-y)\mathrm{p}^2}{(y\mathrm{p}' + (1-y)\mathrm{p})^2}, \tag{B17}$$

$\mathrm{q} = \mathrm{p}' - \mathrm{p}$. The coefficients C_{ij} can be expressed in terms of C_0, as it was done in Ref. [7], and the coefficient C_0 can be evaluated in terms of the Spence function (dilogarithm) [19]. However, we found that safer to perform the integration over the Feynman parameter y numerically.

Evaluating the integral over y in Eqs. (B12)–(B15), one should remember that the denominator $(y\mathrm{p}' + (1-y)\mathrm{p})^2$ can have zeros on the interval of the integration. It does not cause any singularities because of corresponding zeros of the numerator. However, one should take care of numerical cancellations arising in the vicinity of these points. This was handled by dividing the integration interval into two or three pieces according to the number of the zeros.

For the calculation of the one-potential term, only the time component of the vertex function $\Gamma^{\mu}_R(\mathrm{p}',\mathrm{p})$ is needed. To perform the angular integration in the one-potential term, it is convenient to write $\overline{\psi}(\mathbf{p}')\Gamma^0_R(\mathrm{p}',\mathrm{p})\psi(\mathbf{p})$ in the form

$$\overline{\psi}_a(\mathbf{p}')\Gamma^0_R(\mathrm{p}',\mathrm{p})\psi_a(\mathbf{p}) = \frac{\alpha}{4\pi}\{\mathcal{F}_1\chi^{\dagger}_{\kappa_a\mu_a}(\hat{\mathbf{p}}')\chi_{\kappa_a\mu_a}(\hat{\mathbf{p}}) + \mathcal{F}_2\chi^{\dagger}_{-\kappa_a\mu_a}(\hat{\mathbf{p}}')\chi_{-\kappa_a\mu_a}(\hat{\mathbf{p}})\}. \tag{B18}$$

One can see that the functions $\mathcal{F}_{1,2}$ can be expressed as follows:

$$\mathcal{F}_1(p',p,\xi) = A\tilde{g}'\tilde{g} + \varepsilon_a(B_1+B_2)(\varepsilon_a\tilde{g}' + p'\tilde{f}')\tilde{g} + \varepsilon_a(C_1+C_2)\tilde{g}'(\varepsilon_a\tilde{g} + p\tilde{f}) + D(\varepsilon_a\tilde{g}' + p'\tilde{f}') \times(\varepsilon_a\tilde{g} + p\tilde{f}) + \varepsilon_a(H_1+H_2)\tilde{g}'\tilde{g}, \tag{B19}$$

$$\mathcal{F}_2(p',p,\xi) = A\tilde{f}'\tilde{f} + \varepsilon_a(B_1+B_2)(\varepsilon_a\tilde{f}' + p'\tilde{g}')\tilde{f} + \varepsilon_a(C_1 + C_2)\tilde{f}'(\varepsilon_a\tilde{f} + p\tilde{g}) + D(\varepsilon_a\tilde{f}' + p'\tilde{g}') \times(\varepsilon_a\tilde{f} + p\tilde{g}) - \varepsilon_a(H_1+H_2)\tilde{f}'\tilde{f}, \tag{B20}$$

where $p=|\mathbf{p}|$, $p'=|\mathbf{p}'|$, $\xi=\cos(\widehat{\mathbf{pp}'})$, $\tilde{g}$ and $\tilde{f}$ denote the components of the wave function in the momentum representation (6): $\tilde{g}=\tilde{g}_a(p)$, $\tilde{f}=\tilde{f}_a(p)$, $\tilde{g}'=\tilde{g}_a(p')$, and $\tilde{f}'=\tilde{f}_a(p')$; $\varepsilon_a=\mathrm{p}_0=\mathrm{p}_0'$ is the energy of the initial state.

APPENDIX C: RADIAL INTEGRAL $R_J(\omega,ABCD)$

The evaluation of the integral $R_J(\omega,abcd)$ defined by Eq. (23) can be found in Ref. [16]. For our purposes it is convenient to write it in the forms

$$R_J(\omega,abcd)=(2J+1)\int_0^\infty x_2^2dx_2x_1^2dx_1 \times\Big\{(-1)^J C_J(\kappa_a,\kappa_c)C_J(\kappa_b,\kappa_d) \times g_J(\omega,x_<,x_>)W_{ac}(x_1)W_{bd}(x_2) -\sum_L (-1)^L g_L(\omega,x_<,x_>)X_{ac}(x_1)X_{bd}(x_2)\Big\}, \tag{C1}$$

$$W_{ab}(x)=g_a(x)g_b(x)+f_a(x)f_b(x), \tag{C2}$$

$$X_{ab}(x)=g_a(x)f_b(x)S_{JL}(-\kappa_b,\kappa_a)-f_a(x)g_b(x) \times S_{JL}(\kappa_b,-\kappa_a), \tag{C3}$$

where g_n and f_n are the upper and lower radial components of the Dirac wave function, respectively, $x_>=\max(x_1,x_2)$, and $x_<=\min(x_1,x_2)$. The function $g_l(\omega,x_<,x_>)$ is the radial part of the partial wave expansion of the photon propagator:

$$\frac{e^{i\omega x_{12}}}{x_{12}}=\sum_l (2l+1)g_l(\omega,x_<x_>)P_l(\cos(\widehat{\mathbf{x}_1\mathbf{x}_2})), \tag{C4}$$

$$g_l(0,x_<x_>)=\frac{1}{2l+1}\frac{x_<^l}{x_>^{l+1}}, \tag{C5}$$

$$g_l(\omega,x_<x_>)=i\omega j_l(\omega x_<)h_l^{(1)}(\omega x_>), \tag{C6}$$

where $P_l(z)$ is the Legendre polynomial, and $j_l(z)$ and $h_l^{(1)}(z)$ are the spherical Bessel functions.

The angular coefficients $S_{JL}(\kappa_a,\kappa_b)$ differ from the zero only for $L=J-1,J,J+1$, and can be written for $J\neq 0$ as follows:

$$S_{J\,J+1}(\kappa_a,\kappa_b)=\sqrt{\frac{J+1}{2J+1}}\left(1+\frac{\kappa_a+\kappa_b}{J+1}\right)C_J(-\kappa_b,\kappa_a), \tag{C7}$$

$$S_{J\,J}(\kappa_a,\kappa_b)=\frac{\kappa_a-\kappa_b}{\sqrt{J(J+1)}}C_J(\kappa_b,\kappa_a), \tag{C8}$$

$$S_{J\,J-1}(\kappa_a,\kappa_b)=\sqrt{\frac{J}{2J+1}}\left(-1+\frac{\kappa_a+\kappa_b}{J}\right)C_J(-\kappa_b,\kappa_a). \tag{C9}$$

In the case when $J=0$ there is only one nonvanishing coefficient $S_{01}(\kappa_a,\kappa_b)=C_0(-\kappa_b,\kappa_a)$. The coefficients $C_J(\kappa_b,\kappa_a)$ are given by the expression

$$C_J(\kappa_b,\kappa_a)=(-1)^{j_b+1/2}\sqrt{(2j_a+1)(2j_b+1)} \times\begin{pmatrix} j_a & J & j_b \\ \frac{1}{2} & 0 & -\frac{1}{2}\end{pmatrix}\Pi(l_a,l_b,J), \tag{C10}$$

the symbol $\Pi(l_a,l_b,J)$ is unity if l_a+l_b+J is even, and zero otherwise.

APPENDIX D: COMPUTATION OF THE $G_\kappa^{(2+)}$ FUNCTION

For the calculation of the many-potential term (26) it is necessary to compute a part of the electron propagator with two or more Coulomb interactions inserted:

$$G^{2+}(\omega)=\frac{1}{\omega-\mathcal{H}_0}V\frac{1}{\omega-\mathcal{H}}V\frac{1}{\omega-\mathcal{H}_0}. \tag{D1}$$

The function $G^{2+}(\omega,\mathbf{x}_1,\mathbf{x}_2)$ has the same angular dependence as the Dirac-Coulomb Green function and can be written in the form

$$G^{2+}(\omega,\mathbf{x}_1,\mathbf{x}_2)=\sum_{\kappa\mu}\begin{pmatrix} (G_\kappa^{2+})_{11}\chi_{\kappa\mu}(\hat{\mathbf{x}}_1)\chi_{\kappa\mu}^\dagger(\hat{\mathbf{x}}_2) & -i(G_\kappa^{2+})_{12}\chi_{\kappa\mu}(\hat{\mathbf{x}}_1)\chi_{-\kappa\mu}^\dagger(\hat{\mathbf{x}}_2) \\ i(G_\kappa^{2+})_{21}\chi_{-\kappa\mu}(\hat{\mathbf{x}}_1)\chi_{\kappa\mu}^\dagger(\hat{\mathbf{x}}_2) & (G_\kappa^{2+})_{22}\chi_{-\kappa\mu}(\hat{\mathbf{x}}_1)\chi_{-\kappa\mu}^\dagger(\hat{\mathbf{x}}_2)\end{pmatrix}. \tag{D2}$$

We refer to the radial part of the term of the κ expansion of $G^{2+}(\omega,\mathbf{x}_1,\mathbf{x}_2)$ as $\mathbf{G}_\kappa^{2+}(\omega,x_1,x_2)$:

$$\mathbf{G}_\kappa^{2+}(\omega,x_1,x_2)=\begin{pmatrix}(G_\kappa^{2+})_{11} & (G_\kappa^{2+})_{12} \\ (G_\kappa^{2+})_{21} & (G_\kappa^{2+})_{22}\end{pmatrix}. \tag{D3}$$

For the numerical evaluation of the $\mathbf{G}_\kappa^{2+}(\omega,x_1,x_2)$ function we subtract from the radial Dirac-Coulomb Green function the two first terms of the Taylor expansion at the point $Z=0$ (Z is the nuclear charge number):

$$\mathbf{G}_\kappa^{(2+)}(\omega,x_1,x_2)=\mathbf{G}_\kappa(\omega,x_1,x_2)-\mathbf{G}_\kappa^{(0)}(\omega,x_1,x_2) -\mathbf{G}_\kappa^{(1)}(\omega,x_1,x_2), \tag{D4}$$

where $\mathbf{G}_\kappa(\omega,x_1,x_2)$ is the radial Dirac-Coulomb Green function:

$$\mathbf{G}_\kappa^{(0)}(\omega,x_1,x_2)=\mathbf{G}_\kappa(\omega,x_1,x_2)\big|_{Z=0}, \tag{D5}$$

$$\mathbf{G}_\kappa^{(1)}(\omega,x_1,x_2)=Z\left[\frac{d}{dZ}\mathbf{G}_\kappa(\omega,x_1,x_2)\right]\Big|_{Z=0}. \tag{D6}$$

The computation of the $\mathbf{G}_\kappa^{(2+)}$ function was performed in a wide range of real values of x_1 and x_2, complex values of ω ($\Re(\omega)\leqslant 1$), and $|\kappa|\leqslant 50$. The achieved numerical precision is estimated to be better than 10^{-8} in most cases.

1. Dirac-Coulomb Green function

The radial Green function of the Dirac equation can be written in the form:

$$\mathbf{G}_\kappa(\omega,x_1,x_2)=-\frac{1}{\Delta_\kappa(\omega)}[\boldsymbol{\phi}_\kappa^\infty(\omega,x_1)\boldsymbol{\phi}_\kappa^{0\mathrm{T}}(\omega,x_2)\times\theta(x_1-x_2)+\boldsymbol{\phi}_\kappa^0(\omega,x_1)\boldsymbol{\phi}_\kappa^{\infty\mathrm{T}}(\omega,x_2)\times\theta(x_2-x_1)], \tag{D7}$$

where $\boldsymbol{\phi}_\kappa^0$ and $\boldsymbol{\phi}_\kappa^\infty$ are the solutions of the radial Dirac equation, bounded at the origin and at the infinity, respectively. $\Delta_\kappa(\omega)$ is the Wronskian:

$$\Delta_\kappa(\omega)=x^2\boldsymbol{\phi}_\kappa^{0\mathrm{T}}(\omega,x)\begin{pmatrix}0&-1\\1&0\end{pmatrix}\boldsymbol{\phi}_\kappa^\infty(\omega,x). \tag{D8}$$

For the pure Coulomb potential the radial Dirac equation can be solved analytically in the form [15]

$$\boldsymbol{\phi}_\kappa^0(\omega,x)=\begin{pmatrix}\phi_\kappa^{0,+}(\omega,x)\\ \phi_\kappa^{0,-}(\omega,x)\end{pmatrix}, \tag{D9}$$

$$\boldsymbol{\phi}_\kappa^\infty(\omega,x)=\begin{pmatrix}\phi_\kappa^{\infty,+}(\omega,x)\\ \phi_\kappa^{\infty,-}(\omega,x)\end{pmatrix}, \tag{D10}$$

$$\phi_\kappa^{0,\pm}(\omega,x)=\frac{\sqrt{1\pm\omega}}{x^{3/2}}\left[(\lambda-\nu)M_{\nu-(1/2),\lambda}(2cx)\mp\left(\kappa-\frac{\alpha Z}{c}\right)M_{\nu+(1/2),\lambda}(2cx)\right], \tag{D11}$$

$$\phi_\kappa^{\infty,\pm}(\omega,x)=\frac{\sqrt{1\pm\omega}}{x^{3/2}}\left[\left(\kappa+\frac{\alpha Z}{c}\right)W_{\nu-(1/2),\lambda}(2cx)\pm W_{\nu+(1/2),\lambda}(2cx)\right], \tag{D12}$$

$$\Delta_\kappa(\omega)=4c^2\frac{\Gamma(1+2\lambda)}{\Gamma(\lambda-\nu)}, \tag{D13}$$

where $c=\sqrt{1-\omega^2}$ ($\Re(c)>0$), $\lambda=\sqrt{\kappa^2-(\alpha Z)^2}$, $\nu=\alpha Z\omega/c$, and $M_{\alpha,\beta}$ and $W_{\alpha,\beta}$ are the Whittaker functions of the first and second kind, respectively. Their computation is described in Appendix E.

Often in atomic structure calculations it is necessary to take into account the effect of the finite nuclear size. In this case one should calculate the Green function of the Dirac equation with the potential of an extended nucleus. Numerical algorithms for the computation of the Dirac Green function in the case of a homogeneously charged sphere and a hollow shell nuclear models were developed by Mohr and co-workers and are described in [17].

2. Calculation of the $\mathbf{G}_\kappa^{(1)}$ function

The direct differentiation of the expressions (D7)–(D13) according to the definition of the $\mathbf{G}_\kappa^{(1)}$ function (D6) yields, for $x_2>x_1$,

$$\mathbf{G}_\kappa^{(1)}(\omega,x_1,x_2)=-\frac{\alpha Z}{\Delta_\kappa^{(0)}}\frac{\omega}{c}\{[\delta\boldsymbol{\phi}_\kappa^0(\omega,x_1)]_0[\boldsymbol{\phi}_\kappa^\infty(\omega,x_2)]_0^{\mathrm{T}}+[\boldsymbol{\phi}_\kappa^0(\omega,x_1)]_0[\delta\boldsymbol{\phi}_\kappa^\infty(\omega,x_2)]_0^{\mathrm{T}}-\psi(|\kappa|)\times[\boldsymbol{\phi}_\kappa^0(\omega,x_1)]_0[\boldsymbol{\phi}_\kappa^\infty(\omega,x_2)]_0^{\mathrm{T}}\}. \tag{D14}$$

For $x_2<x_1$ the $\mathbf{G}_\kappa^{(1)}(\omega,x_1,x_2)$ function can be obtained from Eq. (D14) together with the symmetry condition $\mathbf{G}_\kappa^{(1)}(\omega,x_1,x_2)=\mathbf{G}_\kappa^{(1)\mathrm{T}}(\omega,x_2,x_1)$.

The components of the $\boldsymbol{\phi}_\kappa$, $\delta\boldsymbol{\phi}_\kappa$ functions are

$$[\phi_\kappa^{0,\pm}(\omega,x)]_0=\frac{\sqrt{1\pm\omega}}{x^{3/2}}[|\kappa|M_-\mp\kappa M_+], \tag{D15}$$

$$[\phi_\kappa^{\infty,\pm}(\omega,x)]_0=\frac{\sqrt{1\pm\omega}}{x^{3/2}}[\kappa W_-\pm W_+], \tag{D16}$$

$$[\delta\phi_\kappa^{0,\pm}(\omega,x)]_0=\frac{\sqrt{1\pm\omega}}{x^{3/2}}\left[(-M_-+|\kappa|M'_-)\mp\left(-\frac{1}{\omega}M_+ +\kappa M'_+\right)\right], \tag{D17}$$

$$[\delta\phi_\kappa^{\infty,\pm}(\omega,x)]_0=\frac{\sqrt{1\pm\omega}}{x^{3/2}}\left[\left(\frac{1}{\omega}W_-+\kappa W'_-\right)\pm W'_+\right], \tag{D18}$$

$$\Delta_\kappa^{(0)}(\omega)=4c^2\frac{(2|\kappa|)!}{(|\kappa|-1)!}, \tag{D19}$$

where

$$M_\pm=M_{\pm 1/2,|\kappa|}(2cx),\ W_\pm=W_{\pm 1/2,|\kappa|}(2cx),$$

$$M'_\pm=(d/d\nu)M_{\nu\pm 1/2,|\kappa|}(2cx)|_{\nu=0},$$

$$W'_\pm=(d/d\nu)W_{\nu\pm 1/2,|\kappa|}(2cx)|_{\nu=0},$$

and $\psi(x)$ is the logarithmic derivative of the Γ function. The numerical algorithms for the evaluation of the $M'_{\pm}$ and $W'_{\pm}$ functions are described in Appendix F.

APPENDIX E: NUMERICAL EVALUATION OF THE WHITTAKER FUNCTIONS

The computation of the Whittaker functions was discussed previously in detail by Mohr [3]. The present numerical evaluation is similar in some aspects to that one. The important difference is that in Ref. [3] the 128-bit arithmetic was used in a certain range of the variation of the argument for the computation of the Whittaker function of the second kind. This makes its numerical evaluation very time consuming. Our method of the numerical evaluation employes only the double precision (64-bit) arithmetic.

1. Computation of the Whittaker function of the first kind

The first solution of Whittaker's differential equation is given by the expression [20]

$$M_{\lambda,\mu}(z)=z^{\mu+(1/2)}e^{-z/2}{}_1F_1(\mu-\lambda+\tfrac{1}{2},2\mu+1;z), \quad \text{(E1)}$$

where ${}_1F_1(a,b;z)$ is the confluent hypergeometric function. $M_{\lambda,\mu}(z)$ can be computed comparatively easily via its definition by summing the hypergeometric series [20]:

$$M_{\lambda,\mu}(z)=z^{\mu+(1/2)}e^{-z/2}\sum_{n=0}^{\infty}\frac{\left(\mu-\lambda+\frac{1}{2}\right)_n}{(2\mu+1)_n}\frac{z^n}{n!}, \quad \text{(E2)}$$

where $(a)_n=\Gamma(a+n)/\Gamma(a)$ is the Pochhammer symbol. The summation in Eq. (E2) can be evaluated up to a desirable precision for small and moderately large arguments, while for large z the numerical overflow arises due to the exponential behavior of $M_{\lambda,\mu}(z)$.

Another method for the computation of the Whittaker function of the first kind was proposed in Ref. [3]. This method is based on the series expansion of the integral representation for $M_{\lambda,\mu}(z)$, and yields the following expression:

$$M_{\lambda-(1/2),\mu}(z)\pm M_{\lambda+(1/2),\mu}(z)=z^{\mu+(1/2)}\sum_{n=0}^{\infty}I_{\pm}(n)\frac{(z/2)^n}{n!}, \quad \text{(E3)}$$

where $I_{\pm}(n)$ are calculated recursively:

$$I_+(n+1)=I_-(n)-\frac{2\lambda}{n+1+2\mu}I_+(n), \quad \text{(E4)}$$

$$I_-(n+1)=\frac{n+1}{n+1+2\mu}I_+(n), \quad \text{(E5)}$$

with $I_+(0)=2, I_-(0)=0$. This algorithm is stable for not very large z as well as the first method.

In the region where $|[\Gamma(2\mu+1)/\Gamma(\mu+\lambda+1/2)]z^{\lambda}e^{-z/2}|<\delta$ (δ is a desired numerical precision), for the computation of $M_{\lambda,\mu}(z)$ one can use the asymptotic expansion in the form [21]

$$M_{\lambda,\mu}(z)=\frac{\Gamma(2\mu+1)}{\Gamma\left(\mu-\lambda+\frac{1}{2}\right)}z^{-\lambda}e^{z/2}\times\sum_{n=0}^{N}\frac{\left(\frac{1}{2}+\mu+\lambda\right)_n\left(\frac{1}{2}-\mu+\lambda\right)_n}{n!}z^{-n}+O(|z^{-(\lambda+N+1)}e^{z/2}|). \quad \text{(E6)}$$

In Eq. (E6) the exponentially growing factor $e^{z/2}$ can be separated and compensated for by a correspondingly small factor from the asymptotic expansion of the function W. In this way the numerical overflow in the computation of the product of two Whittaker functions MW can be avoided for large values of the argument.

2. Computation of the Whittaker function of the second kind

The second solution of Whittaker's differential equation is defined as follows [20]:

$$W_{\lambda,\mu}(z)=\frac{\Gamma(-2\mu)}{\Gamma\left(\frac{1}{2}-\mu-\lambda\right)}M_{\lambda,\mu}(z)+\frac{\Gamma(2\mu)}{\Gamma\left(\frac{1}{2}+\mu-\lambda\right)}M_{\lambda,-\mu}(z). \quad \text{(E7)}$$

When the absolute value of the argument is relatively small, the computation of $W_{\lambda,\mu}(z)$ can be performed directly via its definition. However, large numerical cancellations arise for large arguments. The reason for this is that, as one can see from the asymptotic behavior of the Whittaker functions, the exponentially decreasing function $W_{\lambda,\mu}(z)$ is defined as a sum of two exponentially growing functions.

For large values of the argument the asymptotic expansion can be used [21]:

$$W_{\lambda,\mu}(z)=z^{\lambda}e^{-z/2}\sum_{n=0}^{N}\frac{\left(\frac{1}{2}+\mu-\lambda\right)_n\left(\frac{1}{2}-\mu-\lambda\right)_n}{n!}(-z)^{-n}+O(|z^{\lambda-N-1}e^{-z/2}|). \quad \text{(E8)}$$

In the region of moderate values of $|z|$ and $\mu\leqslant 15$, neither method described above can provide a desirable precision. In this case we use a more sophisticated algorithm proposed by Luke [22] for the computing of the second solution of the confluent hypergeometric differential equation $U(a,c;z)$. The Whittaker function of the second kind can be written in terms of the $U(a,c;z)$ function as follows:

$$W_{\lambda,\mu}(z)=z^{\mu+(1/2)}e^{-z/2}U(\mu-\lambda+\tfrac{1}{2},2\mu+1;z). \quad \text{(E9)}$$

The $U(a,c;z)$ function can be expressed as an expansion over the Chebyschev polynomials:

$$U(a,c;\omega z)=(\omega z)^{-a}\sum_{n=0}^{\infty} C_n(z)T_n^*\left(\frac{1}{\omega}\right), \qquad \text{(E10)}$$

$a,1+a-c\neq 0,-1,-2,\ldots;z\neq 0,|\arg(z)|<3\pi/2$, ω is a free parameter ($\omega\geqslant 1$), $T_n^*(x)=T_n(2x-1)$, and $T_n(x)$ are the Chebyschev polynomials. The coefficients $C_n(z)$ satisfy the recurrent equation

$$\frac{2C_n(z)}{\epsilon_n}=\zeta_n(z)C_{n+1}(z)+\eta_n(z)C_{n+2}(z)+\varsigma_n C_{n+3}(z), \qquad \text{(E11)}$$

$$\zeta_n(z)=2(n+1)\left(1-\frac{(2n+3)(n+a+1)(n+b+1)}{2(n+2)(n+a)(n+b)}-\frac{2z}{(n+a)(n+b)}\right), \qquad \text{(E12)}$$

$$\eta_n(z)=1-\frac{2(n+1)(2n+3-2z)}{(n+a)(n+b)}, \qquad \text{(E13)}$$

$$\varsigma_n=-\frac{(n+1)(n+3-a)(n+3-b)}{(n+2)(n+a)(n+b)}, \qquad \text{(E14)}$$

where $b=1+a-c$, $\epsilon_0=1$, $\epsilon_n=2$ for $n\geqslant 1$. Expressions (E11)–(E14), together with the normalization relation for the coefficients $C_n(z)$,

$$\sum_{n=0}^{\infty}(-1)^n C_n(z)=1, \qquad \text{(E15)}$$

provide a convenient method for the numerical evaluation of expansion (E10) assuming the sum converges; therefore, $\lim_{n\to\infty} C_n(z)=0$. To evaluate the sum, the natural N was chosen to be large enough for one to assume $C_{N+1}(z)=0$ and $C_{N+2}(z)=0$. We start with $C_N(z)=1$ and employ the recurrence equation (E11) downwards. Then we normalize the coefficients $C_n(z)$ using expression (E15), and perform the summing of the Chebyschev polynomials. The sum of the Chebyschev polynomials can be easily evaluated using the well-known recurrent relations (see, e.g., Ref. [22]). To estimate the uncertainty of the numerical evaluation, one can enlarge N and repeat the procedure until the difference between the results of the evaluation becomes smaller than the desirable numerical uncertainty.

Recently a method for the computation of the $W_{\lambda,\mu}(z)$ function was reported based on a nonlinear sequence transformation of the asymptotic series expansion of $W_{\lambda,\mu}(z)$ [23]. The region of the application of the algorithm is found to be close to the previous one, thus this method was not used in the actual numerical calculations.

For the computation of the $\mathbf{G}_\kappa^{(1)}(\omega,x_1,x_2)$ function (D14), one should calculate $W_{\lambda,\mu}(z)$ with 2λ and μ are integer. In this case the following expression can be used [21]:

$$W_{\lambda,\mu}(z)=z^{\mu+1/2}e^{-z/2}\left\{\frac{(2\mu-1)!}{\Gamma(1/2+\mu-\lambda)}\sum_{m=0}^{2\mu-1}\frac{(1/2-\mu-\lambda)_m}{(1-2\mu)_m}\frac{z^{m-2\mu}}{m!}+\frac{(-1)^{2\mu}}{(2\mu)!\Gamma(1/2-\mu-\lambda)}\sum_{m=0}^{\infty}\frac{(1/2+\mu-\lambda)_m}{(2\mu+1)_m}\frac{z^m}{m!}\right.$$
$$\left.\times[\psi(1+m)+\psi(2\mu+1+m)-\psi(1/2+\mu-\lambda+m)-\ln z]\right\}, \qquad \text{(E16)}$$

which is valid when $2\mu+1$ is an integer.

We are interested only in certain values of the parameters: $\lambda=\pm\frac{1}{2}$, and μ is an integer. In this case expression (E16) simplifies greatly:

$$W_{1/2-n,k}(z)=z^{-k+1/2}e^{-z/2}\frac{1}{\Gamma(k+n)}\sum_{m=0}^{k-n}\frac{\Gamma(2k-m)}{(k-n+1)_{-m}}\frac{z^m}{m!}, \qquad \text{(E17)}$$

here $n=0,1$.

APPENDIX F: COMPUTATION OF THE DERIVATIVES OF THE WHITTAKER FUNCTIONS

In this section we discuss the computation of the derivatives of Whittaker functions of the special kind: $(d/d\eta)M_{\eta\pm 1/2,k}(z)|_{\eta=0}$ and $(d/d\eta)W_{\eta\pm 1/2,k}(z)|_{\eta=0}$. We use the notations $M'_{\pm 1/2,k}(z)$ and $W'_{\pm 1/2,k}(z)$, respectively, for these derivatives.

The computation of these derivatives of the Whittaker functions was studied previously in Ref. [24]. The present numerical evaluation is similar to that one with some changes in computation of $W'_{\pm 1/2,k}(z)$. For the sake of completeness we reproduce formulas from Ref. [24] below with some misprints corrected.

1. Computation of the derivatives of the Whittaker function of the first kind

The term-by-term differentiation of the hypergeometric series (E2) yields

$$M'_{1/2-n,k}(z)=e^{-z/2}\sum_{m=1}^{\infty}\frac{(n+k)_m}{(2k+1)_m}\frac{z^{m+k+1/2}}{m!}(\psi(n+k)-\psi(n+k+m)). \qquad \text{(F1)}$$

In the region where $|[\Gamma(2k+1)/\Gamma(k-n+1)]z^{1/2-n}e^{-z/2}\ln z|<\delta$ (δ is a desired numerical precision), the asymptotic expansion for $M'_{1/2-n,k}(z)$ was used in the form

$$M'_{1/2-n,k}(z)=e^{z/2}\left\{\frac{\Gamma(2k+1)}{\Gamma(k+n)}\sum_{m=0}^{k+n-1}(-1)^m\frac{(k-n+1)_m}{(k+n)_{-m}}\frac{z^{-m+n-1/2}}{m!}(\psi(k-n+m+1)-\psi(k-n+1)+\psi(k+n-m)-\ln z)\right.$$
$$\left.-\frac{[(2k)!]^2(-1)^{k+n}}{(k-n)!(k+n)!}\sum_{m=0}^{\infty}\frac{(2k+1)_m}{(k+n+1)_m}\frac{m!}{z^{k+m+1/2}}\right\}. \tag{F2}$$

As series (F2) is an asymptotic row, it is divergent. Despite this fact, it can be used for the numerical computation provided the summation is properly terminated.

2. Computation of the derivatives of the Whittaker function of the second kind

The term-by-term differentiation of expression (E16) yields

$$W'_{1/2-n,k}(z)=e^{-z/2}\left\{\frac{(-1)^{k+n}(k-n)!}{(2k)!}\sum_{m=0}^{\infty}\frac{(k+n)_m}{(2k+1)_m}\frac{z^{m+k+1/2}}{m!}(\ln z-\psi(m+1)+\psi(k+n+m)-\psi(2k+m+1))\right.$$
$$+\sum_{m=0}^{k-n}\frac{(k+n)_m(k-n-m+1)_m}{m!z^{n+m-1/2}}(\psi(k+n)+\psi(k-n+1)-\psi(m+1))$$
$$\left.+\sum_{m=0}^{k+n-2}\frac{(-1)^m m!z^{m-n+3/2}}{(k-n+1)_{m+1}(k+n-m-1)_{m+1}}\right\}. \tag{F3}$$

This expression becomes numerically unsafe for large values of the argument due to large numerical cancellations between terms of the sum.

For large arguments one can use the asymptotic expansion of $W'_{1/2-n,k}(z)$:

$$W'_{1/2-n,k}(z)=e^{-z/2}\left\{\sum_{m=0}^{k-n}\frac{(k+n)_m(k-n-m+1)_m}{m!z^{n+m-1/2}}\right.$$
$$\left.\times\left[\sum_{l=0}^{m-1}\left(\frac{1}{k-n-l}-\frac{1}{k+n+l}\right)+\ln z\right]-\sum_{m=k-n+1}^{\infty}\frac{(-1)^{m+k-n}(k+n)_m(k-n)!}{(m+n-k)_{k-n+1}z^{m+n-1/2}}\right\}, \tag{F4}$$

where the second sum should be properly terminated due to the asymptotic nature of the expansion.

For moderate arguments and $k\leqslant 15$, the accuracy of these methods becomes quite poor. Thus we have to employ the numerical differentiation of the $W_{\lambda,\mu}(z)$ function obtained with formulas (E9)–(E15) to achieve a desirable precision in this region.

[1] A. M. Desiderio and W. R. Johnson, Phys. Rev. A **3**, 1287 (1971).
[2] G. E. Brown, J. S. Langer, and G. W. Schafaer, Proc. R. Soc. London, Ser. A **251**, 92 (1959).
[3] P. J. Mohr, Ann. Phys. (N.Y.) **88**, 26 (1974); **88**, 52 (1974).
[4] P. J. Mohr, Phys. Rev. A **46**, 4421 (1992).
[5] P. J. Mohr and Y. K. Kim, Phys. Rev. A **45**, 2727 (1992).
[6] P. J. Mohr and G. Soff, Phys. Rev. Lett. **70**, 158 (1993).
[7] N. J. Snyderman, Ann. Phys. (N.Y.) **211**, 43 (1991).
[8] S. A. Blundell and N. J. Snyderman, Phys. Rev. A **44**, R1427 (1991).
[9] H. Persson, I. Lindgren, and S. Salomonson, Phys. Scr. **T46**, 125 (1993).
[10] H. M. Quiney and I. P. Grant, Phys. Scr. **T46**, 132 (1993); J. Phys. B **27**, L299 (1994).
[11] V. A. Yerokhin, A. N. Artemyev, and V. M. Shabaev, Phys. Lett. A **234**, 361 (1997); V. A. Yerokhin, A. N. Artemyev, T. Beier, V. M. Shabaev, and G. Soff, J. Phys. B **31**, L691 (1998).
[12] V. M. Shabaev, M. B. Shabaeva, I. I. Tupitsyn, V. A. Yerokhin, A. N. Artemyev, T. Kühl, M. Tomaseli, and O. M. Zherebtsov, Phys. Rev. A **57**, 149 (1998); **58**, 1610 (1998).
[13] E. M. Rose, *Relativistic Electron Theory* (Wiley, New York, 1961).
[14] M. Baranger, H. A. Bethe, and R. P. Feynman, Phys. Rev. **92**, 482 (1953).
[15] E. H. Whichmann and N. M. Kroll, Phys. Rev. **101**, 843 (1956).
[16] W. R. Johnson, S. A. Blundell, and J. Sapirstein, Phys. Rev. A **37**, 2764 (1988).
[17] P. J. Mohr, G. Plunien, and G. Soff, Phys. Rep. **293**, 227 (1998).
[18] P. Indelicato and P. J. Mohr, Phys. Rev. A **58**, 165 (1998).
[19] G. 't Hooft and M. Veltman, Nucl. Phys. B **153**, 365 (1979).
[20] I. S. Gradshtein and I. M. Ryzhik, *Table of Integrals, Series and Products* (Academic, New York, 1980).
[21] H. Bateman and A. Erdélyi, *Higher Transcendental Functions* (McGraw-Hill, New York, 1953).
[22] Y. L. Luke, *Mathematical Functions and Their Approximations* (Academic, New York, 1975).
[23] E. J. Weniger, Comput. Phys. **10**, 496 (1996).
[24] N. L. Manakov, A. A. Nekipelov, and A. G. Fainstein, Zh. Eksp. Teor. Fiz. **95**, 1167 (1989) [Sov. Phys. JETP **68**, 673 (1989)].